

# **Statistics of extremes and estimation of extreme rainfall**

## **2. Empirical investigation of long rainfall records**

Demetris Koutsoyiannis

Department of Water Resources, Faculty of Civil Engineering, National Technical University of Athens, Heroon Polytechneiou 5, GR-157 80 Zographou, Greece (dk@itia.ntua.gr)

**Abstract** In the first part of this study, theoretical analyses showed that the Gumbel distribution is quite unlikely to apply to hydrological extremes and that the extreme value distribution of type II (EV2) is a more consistent choice. Based on these theoretical analyses, an extensive empirical investigation is performed using a collection of 169 of the longest available rainfall records worldwide, each having 100-154 years of data. This verifies the theoretical results. In addition, it shows that the shape parameter of the EV2 distribution is constant for all examined geographical zones (Europe and North America), with value  $\kappa = 0.15$ . This simplifies the fitting and the general mathematical handling of the distribution, which become as simple as those of the Gumbel distribution.

**Keywords** design rainfall; extreme rainfall; generalized extreme value distribution; Gumbel distribution; hydrological design; hydrological extremes; probable maximum precipitation; risk.

## **Statistique de valeurs extrêmes et estimation de précipitations extrêmes**

### **2. Recherche empirique sur de longues séries de précipitations**

**Résumé** Dans la première partie de cette étude, des analyses théoriques ont prouvé que la distribution de Gumbel est peu susceptible de s'appliquer aux valeurs extrêmes de variables hydrologiques et que la distribution de valeurs extrêmes du type II (EV2) est un choix plus cohérent. Se basant sur ces analyses théoriques, une recherche empirique étendue est effectuée en utilisant une collection de 169 parmi les séries de précipitations les plus longues qui sont disponibles dans le monde entier, chacun comportant 100-154 ans de données. Ceci

vérifie les résultats théoriques. En outre, on montre que le paramètre de forme de la distribution EV2 est constant pour toutes les zones géographiques examinées (l'Europe et l'Amérique du Nord), avec sa valeur égale à 0.15. Ceci simplifie l'ajustement et la manipulation mathématique générale de la distribution, qui deviennent aussi simples que ceux de la distribution de Gumbel.

**Mots-clés** Précipitations de projet; précipitations extrêmes; distribution généralisée de valeurs extrêmes; Distribution de Gumbel; conception hydrologique; valeurs extrêmes en hydrologie; précipitation maximum probable; risque.

## 1. Introduction

According to the statistical theory of extremes, the distribution function  $H(x)$  of the maximum of a number  $n$  of identically distributed random variables with distribution  $F(x)$ , if  $n$  is large enough (theoretically infinite), takes the asymptotic form, known as the Generalized Extreme Value (GEV) distribution (Jenkinson, 1955, 1969),

$$H(x) = \exp\left\{-\left[1 + \kappa \left(\frac{x}{\lambda} - \psi\right)\right]^{-1/\kappa}\right\}, \quad \kappa x \geq \kappa \lambda (\psi - 1/\kappa) \quad (1)$$

where  $\psi$ ,  $\lambda > 0$  and  $\kappa$  are location, scale and shape parameters, respectively. (Note that the sign convention of  $\kappa$  in (1) is opposite to that most commonly used in hydrological texts and the location parameter is dimensionless).

When  $\kappa = 0$ , the type I distribution of maxima (EV1 or Gumbel distribution),

$$H(x) = \exp[-\exp(-x/\lambda + \psi)] \quad (2)$$

is obtained, which is unbounded from both below and above ( $-\infty < x < +\infty$ ). When  $\kappa > 0$ ,  $H(x)$  represents the extreme value distribution of maxima of type II (EV2), which is bounded from below and unbounded from above ( $\lambda \psi - \lambda/\kappa \leq x < +\infty$ ). A special case, the Fréchet distribution, is obtained when the lower bound becomes zero ( $\psi = 1/\kappa$ ), in which

$$H(x) = \exp\left\{-\left(\frac{\lambda}{\kappa x}\right)^{1/\kappa}\right\}, \quad x \geq 0 \quad (3)$$

When  $\kappa < 0$ ,  $H(x)$  represents the type III (EV3) distribution of maxima. This, however, is of no practical interest in hydrology as it refers to random variables bounded from above ( $-\infty < x \leq \lambda \psi - \lambda/\kappa$ ).

There is a complete correspondence between the distribution of maxima  $H(x)$  and the tail of  $F(x)$ , which can be represented by the distribution of  $x$  conditional on being greater than a certain threshold  $\xi$ , i.e.,  $G(x) := F(x|x > \xi)$ . For appropriate choice of  $\xi$ , it can be shown that (see first part of the study)

$$G(x) = 1 - \left[ 1 + \kappa \left( \frac{x}{\lambda} - \psi \right) \right]^{-1/\kappa}, \quad x \geq \lambda \psi \quad (4)$$

which is the Pareto distribution. For  $\kappa > 0$  this corresponds to the EV2 distribution whereas for  $\kappa = 0$  it takes the form

$$G(x) = 1 - \exp(-x/\lambda + \psi), \quad x \geq \lambda \psi \quad (5)$$

which is the exponential distribution and corresponds to the EV1 distribution. For the special case  $\psi = 1/\kappa$

$$G(x) = 1 - \left( \frac{\lambda}{\kappa x} \right)^{1/\kappa}, \quad x \geq \lambda/\kappa \quad (6)$$

The latter equation, is equivalently written in the power law form  $x = (\lambda/\kappa) T^\kappa$ , where  $T := 1 / [1 - G(x)]$  is the return period. In the generalized Pareto case (4), the corresponding relationship is  $x = (\lambda/\kappa) (T^\kappa - 1 + \kappa \psi)$ .

In hydrological applications,  $H(x)$  is fitted to annual maximum series of a hydrological quantity such as rainfall depth of certain duration, whereas  $G(x)$  is fitted to series of values over threshold (also known as partial duration series) of the same quantity. In the latter case, the threshold is chosen so that the number of events (greater than the threshold) equals the number of years of record.

The EV1 distribution has been the prevailing model for rainfall extremes despite the fact that it results in the highest possible risk for engineering structures, i.e. it yields the smallest possible design rainfall values in comparison to those of the EV2 for any value of the shape parameter. The simplicity of the calculations of the EV1 distribution along with its

geometrical elucidation through a linear probability plot may have contributed to its popularity in hydrologists and engineers. There is also a theoretical justification, as EV1 is the asymptotic extreme value distribution for a wide range of parent distributions that are common in hydrology.

However, the theoretical investigation of part 1 of this study shows that convergence of the exact distribution of maxima to the asymptote EV1 may be extremely slow, thus making the EV1 distribution an inappropriate approximation of the exact distribution of maxima. Besides, the attraction of parent distributions to this asymptote relies on a stationarity assumption, i.e. the assumption that parameters of the parent distribution are constant in time, which may not be the case in hydrological processes. Slight relaxation of this assumption may result in the EV2 rather than the EV1 asymptote.

Simulation experiments of part 1 of this study showed that small sizes of records, e.g. 20-50 years, hide the EV2 distribution and display it as if it were EV1. This allowed the conjecture that the broad use of the EV1 distribution worldwide may in fact be related to small sample sizes rather than to the real behaviour of rainfall maxima, which should be better described by the EV2 distribution. This conjecture is investigated thoroughly here based on real-world long rainfall records.

## **2. Data**

Some thousands of raingauge data sets from Europe and USA were examined in this study, namely data from the United States Historical Climatology Network (USHCN), Land Surface Observation Data of the UK 'Met Office', and data from the oldest stations of France, Italy and Greece. Among these, a total of 169 stations were found to have at least 100 years of data (not including the years with missing data) and were chosen for further analysis. Their geographical locations are shown in Figure 1, classified in six geographical zones. Table 1 shows the general characteristics of raingauges of the different geographical zones and Table 2 gives the general characteristics of the top ten, in terms of record length, raingauges, which are from all countries of this case study (USA, UK, France, Italy and Greece) and are located in four of the six zones.

For all stations, all recorded data values through the station operation were available with the exception of Athens, Greece, where only the annual maximum daily rainfall values were available. From the continuous record of each station (except Athens), two series were extracted, the series of annual maximum values of daily rainfall and the series of values over a threshold chosen so that the number of values equals the number of years of the record. In some of the records there were several missing values or values marked as incorrect, which were deleted. Years with more than five missing daily values in two or more months were excluded. In this way, 169 annual maximum series and 168 series of values over threshold were constructed.

### 3. Initial exploration

As an initial step, the typical statistics and the L-statistics (based on probability-weighted moments; Hosking 1990) were estimated for each annual maximum series of daily rainfall depths. The ranges in each of the six geographical zones and the corresponding averages over all stations of each zone are shown in Table 3. Potential relationships among these statistics and their geographical variation were subsequently explored.

The sample mean ( $\mu$ ) and maximum values ( $x_{\max}$ ) over the observation period of each annual maximum daily rainfall series are plotted in the log-log diagram of Figure 2 using different symbols for each geographical zone. It is observed there that (a) both mean and maximum values vary with the geographical zone (as expected): clouds of points referring to different zones occupy different areas in the diagram; (b) there exists a clear relationship between mean and maximum values (as expected), which seems to be independent of the geographical zone; and (c) this relationship can be approximated by a power law with exponent slightly higher than one (1.08). This is contrary to an observation by Hershfield (1965) that arid areas (with small mean) tend to have higher relative extremes (ratios of maximum to mean or standard deviation) than areas with heavy rainfall. In addition, if Hershfield's observation was valid, it would be manifested as a negative correlation between mean ( $\mu$ ) and coefficient of variation ( $C_v := \sigma/\mu$ , where  $\sigma$  is the standard deviation) or the L-variation ( $\tau_2 := \lambda_2/\mu$ , where  $\lambda_2$  is the second L-moment.). However, Figure 3 does not suggest

such a negative correlation. In fact, the correlation coefficient between  $\mu$  and  $\tau_2$  is +0.30. The correlation coefficient between mean ( $\mu$ ) and L-skewness ( $\tau_3 := \lambda_3/\lambda_2$ , where  $\lambda_3$  is the third L-moment) is slightly positive, too (+0.09, a value not significant statistically).

The dispersion of both  $\tau_2$  and  $\tau_3$  is large as shown in Figure 3. Figure 4, in which  $\tau_3$  is plotted against  $\tau_2$  using different symbols for different geographical zones, shows a positive correlation between  $\tau_2$  and  $\tau_3$  (correlation coefficient = 0.52) and simultaneously indicates independence of the geographical zone, as clouds of points referring to different zones are homogeneously mixed in the diagram. However, the positive correlation between  $\tau_2$  and  $\tau_3$  does not have a physical meaning but rather is a statistical effect. To show this, 169 synthetic samples with lengths and means equal to those of the historical records were generated from the EV2 distribution with constant shape parameter  $\kappa = 0.103$  and location parameter  $\psi = 3.34$  (these values are the averages of the estimated parameters over all stations, as it will be discussed in the next section). The values of the statistics  $\tau_2$  and  $\tau_3$  of these synthetic samples have been plotted in Figure 5, which reveals a picture similar to that of Figure 4 with a strong correlation between  $\tau_2$  and  $\tau_3$  (correlation coefficient = 0.60). Notably, the dispersion of  $\tau_3$  in Figure 5 is identical to that in Figure 4 whereas the dispersion of  $\tau_2$  in the former is slightly smaller than in the latter.

#### 4. Fitting of distribution functions

GEV distributions were fitted to each of the 169 annual maximum series of daily depths using three methods, maximum likelihood, moments and L-moments. The averages over all raingauges and the dispersion characteristics (minimum and maximum values and standard deviations) of the three parameters of the GEV distribution are shown in Table 4. The shape parameter  $\kappa$  is the most important as it determines the type of the distribution of maxima (EV1 or EV2) and consequently the behaviour of the distribution in its tail. Besides, it is the most uncertain parameter as its estimation depends on the skewness ( $C_s$  or  $\tau_3$  for the method of moments or L-moments, respectively) whose value cannot be determined accurately. Clearly, Table 4 shows that in more than 90% of the series the estimated  $\kappa$  is positive, which suggests EV2 distributions. (The smaller values of  $\kappa$  given by the method of moments, as

shown in Table 4, and the smaller percentage of positive values, 74%, is clearly a result of the significant negative bias implied by the estimators of this method, as demonstrated in part 1 of the study). The estimated  $\kappa$  values range between some slightly negative values to over 0.30. Given the observation of the previous section on Figure 5 regarding the statistical behaviour of  $\tau_3$ , which determines  $\kappa$ , it should be expected that the large range of  $\kappa$  values is rather a statistical effect. This will be examined further below.

Figure 6 depicts the EV2 distribution functions fitted by the method of L-moments to the annual maximum series of four of the stations included in the top ten stations of Table 2, namely Charleston City (USA/SC), Oxford (UK), Marseille (France) and Florence (Italy). The estimated shape parameters  $\kappa$  are respectively 0.083, 0.081, 0.155 and 0.120. For comparison, Figure 6 includes also plots of the EV1 distributions fitted again by the method of L-moments and of the empirical distributions determined using Weibull plotting positions. Clearly, the observed maxima for high return periods are higher than the predictions of the EV1 distributions and even from those of the EV2 distribution. Obviously, however the EV2 distribution is in closer agreement to the empirical distribution than the EV1 distribution. The differences of EV1 and EV2 seem to be not very significant for return periods smaller than 50 years.

One may argue that, if the differences between the two distributions are insignificant for return periods smaller than 50 years, then the entire discussion is rather scholastic and not important in engineering design. For example, urban drainage systems are designed for return periods 5-10 years, which for some more important components perhaps can be extended to 50 years. Indeed, for such return periods, the selection of distribution function is not an important issue. In fact, for return periods of 5-10 years there is no need to fit a probabilistic model at all; empirical estimations of probabilities based on the observed maxima suffice, provided that a record with some decades of data is available. The problem becomes essential in the design of major hydraulic constructions such as dam spillways or flood protection works in urban rivers. For example, if a dam is studied for a design duration of  $n = 100$  years and the acceptable risk of the dam overtopping due to flood is  $R = 1\%$ , then the design return period will be (e.g. Chow et al., 1988)  $T = 1/[1 - (1 - R)^{1/n}] \approx 10\,000$  years. Several dams in

Europe have been designed on this probabilistic basis (and not on the doubtful approach of probable maximum precipitation; see discussion in part 1) with return periods of this order of magnitude.

In this respect, the differences of distribution functions, when extrapolated to high return periods such as 1000-100 000 years, are extremely important. These differences are demonstrated graphically in Figure 7, which is similar to the diagrams of Figure 6 but with emphasis given to the tail of the distribution, for return periods higher than 200 years. Figure 7 refers to another station, Athens, Greece, again included in the top ten stations of Table 2. The values of  $\kappa$  estimated by the methods of L-moments, maximum likelihood and moments are respectively 0.170, 0.158 and 0.106. Clearly, the EV1 distribution underestimates seriously the maximum rainfall for high return periods. For instance, at the return period 20 000 years the EV1 distribution results in a value of rainfall depth half that obtained by the EV2 distribution. Another comparison of the two distributions can be done in terms of the value of probable maximum precipitation (PMP). This was initially considered to be the greatest depth of precipitation for a given duration that is physically possible over a geographical location. However, more recently it has been considered as one high rainfall value that has a certain return period like other, higher or lower, values of rainfall depth. Thus, National Research Council (1994, p. 14) assessed that PMP estimates in the USA have return periods of the order  $10^5$  to  $10^9$  and Koutsoyiannis (1999) showed that PMP values estimated by the method of Hershfield have return periods around 60 000 years. The latter method was used by Koutsoyiannis and Baloutsos (2000) to estimate PMP in Athens and resulted in a value of 424.1 mm, which has been plotted in Figure 7. If the return period of this value is estimated by the EV2 distribution, it turns out to be 37 000 to 300 000 years depending on the parameter estimation method whereas EV1 results in the unrealistically high value  $4 \times 10^{10}$  years.

## **5. Study of the variation of parameters**

The problem of the parameter variation and the question whether this variation corresponds to physical (climatological) reasons or is a purely statistical (sampling) effect have been already



posed in the previous sections. Here they will be studied more systematically. As already indicated, simulation is a proper means to assess the sampling effect and estimate the portion of parameter variation that this effect explains. More specifically, a simulation can be performed assuming that one or more statistical parameters are constant. A number of synthetic samples can be thus generated and the sample parameters can be computed. Their variation can then be compared with that of the historical samples.

As already discussed, the variation of the means of the annual maximum series of daily rainfall reflects a climatic variability and is different in different geographical zones. This is also verified by simulation: the standard deviation of means over all stations is 20.0 mm while a simulation assuming constant mean over all stations would yield a standard deviation of only 2.3 mm. This, however, is not the case with other parameters, if they are expressed on a non-dimensionalized basis. Their variability is mostly a sampling effect. To demonstrate this, 169 synthetic samples with lengths and means equal to those of historical series were generated from the GEV distribution with constant shape parameter  $\kappa = 0.103$  and location parameter  $\psi = 3.34$  (dotted lines). These constant values are the averages of the relevant parameters estimated by the method of L-moments (Table 4). The empirical distributions of several dimensionless sample statistics, i.e., coefficients of variation ( $\tau_2$  and  $C_v$ ), skewness ( $\tau_3$  and  $C_s$ ) and kurtosis ( $\tau_4$ ), ratio of maximum value ( $x_{\max}$ ) to mean value ( $\mu$ ), and the parameters  $\kappa$  and  $\psi$  themselves (L-moments estimates), were then obtained and compared graphically to the corresponding empirical distributions obtained from the 169 historical series (Figure 8). It can be observed that in most cases the empirical distributions of the synthetic samples are almost identical to those of the historical ones. The highest differences between the two appear in the distributions of coefficients of variation  $\tau_2$  and  $C_v$ , and that of the location parameter  $\psi$ .

An additional simulation was performed assuming that the parameters  $\kappa$  and  $\psi$  are not constant but random variables uniformly distributed (for simplicity) over an interval, determined so as to match the standard deviation of the parameters shown in Table 4. The resulting empirical distribution functions are also plotted in Figure 8. In all cases, the greater

dispersion of the simulated sampling distributions as compared to the historical ones is apparent.

These simulation experiments and comparisons with historical data suggest that a hypothesis of a common statistical law applying to all 169 series, except for a scaling parameter to account for the different means  $\mu$ , is not far from reality. In this case, a radically improved approach to fitting a probability distribution becomes possible. If the annual maximum daily rainfall series of each station is rescaled by an appropriate scaling factor, then all 18 065 data values can be regarded as realizations of the same statistical law and can be unified in one statistical record. The scaling factor can be the sample mean  $\mu$ . This is an unbiased estimate of the true mean but not the most efficient one. Hershfield (1961) recognising this and attributing it to the fact that outliers in maximum rainfall records may have an appreciable effect on the sample mean, introduced a correction procedure of the sample mean which takes into account a second sample mean computed after excluding the maximum item of the series. Here a similar procedure was devised, which is based on the sample mean  $\mu$  and the maximum item of the series  $x_{\max}$ . A systematic simulation-optimization experiment based on the GEV distribution with  $\kappa$  ranging from 0 to 0.20, showed that the parameter

$$\mu' := \left(1 + \frac{0.94}{n^{0.7}}\right)\mu - \frac{x_{\max}}{n^{0.87}} \quad (7)$$

is an approximately unbiased estimate of the true mean always more efficient than  $\mu$  in the sense that its variance is smaller than that of  $\mu$ . Therefore,  $\mu'$  was used as the rescaling factor.

The empirical distribution of the unified rescaled annual maximum series of daily rainfall is depicted in Figure 9. To this, the EV2 distribution is fitted by several methods and also plotted in Figure 9 whereas its parameters are shown in Table 5. It is observed that the methods of maximum likelihood, moments and L-moments result in (a) different parameter estimates despite the extremely large record length (18 065 station-years), and (b) estimates of distribution quantiles that are systematically lower than the empirical estimates in the tail (for return periods  $> 500$  years). Both these observations may indicate that the EV2 distribution is an imperfect model for annual series of extreme rainfall. However problem (b) can be

resolved by adopting a different parameter estimation method that gives more emphasis to the highest values. Here a weighted least squares method was used, which minimizes the weighted average of square errors between empirical and EV2 quantiles. To give higher importance to the high values, the weights were assumed equal to the empirical quantiles. As shown in Table 5, the latter method resulted in a shape parameter  $\kappa = 0.15$ , greater than those of the other methods. The plot of the EV2 distribution with this shape parameter, shown in Figure 9, is in closer agreement with the empirical distribution in the tail, if compared to those of the other methods, which is very important from an engineer's point of view.

It should be noted that the shape parameter  $\kappa = 0.15$ , whose estimation has given higher importance to the high observed values, may have a negative effect in predictions of the EV2 distribution at short return periods, due to the imperfection of the this distribution. Specifically, it may be anticipated that for return periods of 5-10 years, the EV2 distribution with  $\kappa = 0.15$  may result in underestimation of the rainfall extremes. Therefore, it can be advisable that, if only short return periods are of interest, then the value  $\kappa = 0.10$  should be used, which corresponds to both the L-moments and the maximum likelihood estimations.

In addition to EV2, the EV1 distribution with parameters fitted by the method of L-moments ( $\lambda = 0.283$ ,  $\psi = 2.99$ ) was plotted in Figure 9. Its inappropriateness for return periods greater than 50 years is more than obvious. The weighted least squares method applied to the EV1 distribution results in even worse situation as in the attempt to approach the greatest quantiles the distribution fit becomes poor even in the low distribution quantiles.

In the above analysis, both dimensionless parameters  $\kappa$  and  $\psi$  where hypothesized constant for all stations. A hypothesis somewhat closer to reality would be to introduce some variation to the location parameter  $\psi$  and keep only the parameter  $\kappa$  constant. It is interesting to investigate whether this affects the estimate of the parameter  $\kappa$ . For this investigation, another standardization of the samples was done, so that each data value  $x_{ij}$  (with  $i$  indicating the station and  $j$  the year) is linearly transformed to  $x'_{ij} := (\sigma/\mu) [(x_{ij} - \mu_i)/\sigma_i] + 1$ , where  $\mu_i$  and  $\sigma_i$  are, respectively, the mean and standard deviation of station  $i$ , and  $\mu$  and  $\sigma$  the averages for all stations of the corresponding quantities. Were the value of  $\psi$  constant for all stations, the coefficients of variations  $\sigma_i/\mu_i$  would be constant, too, so the transformation would become

$x'_{ij} := x_{ij}/\mu_i$ , which is the rescaling transformation that was already done in the previous analysis. Similarly to the previous analysis, the corrected mean (equation (7)) was used while for standard deviations the corrections due to Hershfield (1961) were applied.

The so transformed samples of the different stations were again unified and from the unified series the parameters were re-estimated. Interestingly, all parameter estimation methods resulted in virtually the same values of  $\kappa$  that are shown in Table 5 (the largest difference was  $\pm 0.001$ ). Moreover, the parameters  $\lambda$  and  $\psi$  were, too, almost equal to those of Table 5 (largest difference  $\pm 2\%$ ).

## 6. Analysis of series of values over threshold

All previous analyses were performed on the annual maximum series. As discussed in the Introduction, the probabilistic behaviour of the series over threshold can be theoretically obtained from that of the annual maximum series. Here we show that this is also empirically verified. The 168 series were rescaled by  $\mu'$  as obtained from the annual maximum series and then merged into a unified record. The empirical distribution of the unified record is shown in the Pareto probability plot of Figure 10. The Pareto reduced variate that is used for the horizontal axis is defined as  $y_T := (T^\kappa - 1) / \kappa$  with  $\kappa$  fixed to 0.15. The Pareto and exponential distributions with parameters equal to those of the EV2 and EV1 distributions, respectively, shown in Table 5, are also plotted in Figure 10. This figure shows that the same parameters estimated from the unified annual maximum series are good for the Pareto distribution of the unified series of values over threshold, so there is no need to re-estimate them. In addition, the observations already made on Figure 9 about the superiority of the EV2 distribution fitted by the method of least squares and the inappropriateness of the EV1 distribution are valid also for, respectively, the Pareto and exponential distributions in Figure 10.

In addition to the Pareto probability plot of Figure 10, a log-log plot of rescaled rainfall depth versus return period is given in Figure 11. The fact that both the empirical and fitted theoretical distribution functions have an apparent curvature on this log-log plot suggest that the power law relationship between rainfall depth and return period on a basis of values over threshold (which has been called by Turcotte (1994) a fractal distribution and is equivalent to

the Fréchet distribution on a basis of annual maximum values) is inappropriate for modelling rainfall extremes.

## 7. From EV1 to EV2 distribution

All above analyses converge to the conclusion that neither of the two-parameter special cases of the GEV distribution, i.e. the Gumbel and Fréchet distributions, is appropriate for extreme rainfall. On the contrary, the three-parameter EV2 distribution is an alternative much closer to reality. In addition, they converge to the conclusion that the shape parameter of the EV2 distribution can be hypothesized to have a constant value  $\kappa = 0.15$ , regardless of the geographical location of the raingauge station.

If the shape parameter of the EV2 distribution is fixed, the general handling of the distribution becomes as simple as that of the EV1 distribution. For example, the estimation of the remaining two parameters becomes similar to that of the EV1 distribution. That is, the scale parameter can be estimated by the method of moments from

$$\lambda = c_1 \sigma \quad (8)$$

where  $c_1 = \kappa / \sqrt{\Gamma(1 - 2\kappa) - \Gamma^2(1 - \kappa)}$  or  $c_1 = 0.61$  for  $\kappa = 0.15$ , while in the EV1 case  $c_1 = 0.78$ . The relevant estimate for the method of L-moments is

$$\lambda = c_2 \lambda_2 \quad (9)$$

where  $c_2 = \kappa / [\Gamma(1 - \kappa)(2^\kappa - 1)]$  or  $c_2 = 1.23$  for  $\kappa = 0.15$ , while in the EV1 case  $c_2 = 1.443$ . The estimate of the location parameter for both the method of moments and L-moments is

$$\psi = \mu/\lambda - c_3 \quad (10)$$

where  $c_3 = [\Gamma(1 - \kappa) - 1] / \kappa$  or  $c_3 = 0.75$  for  $\kappa = 0.15$ , while in the EV1 case  $c_3 = 0.577$ .

If, in addition to  $\lambda$  and  $\psi$ , the shape parameter is to be estimated directly from the sample (which is not advisable but it may be useful for comparisons) the following equations can be used, which are approximations of the exact (but implicit) equations of the literature:

$$\kappa = \frac{1}{3} - \frac{1}{0.31 + 0.91 C_s + \sqrt{(0.91 C_s)^2 + 1.8}} \quad (11)$$

$$\kappa = 8 c - 3 c^2, \quad c := \frac{\ln 2}{\ln 3} - \frac{2}{3 + \tau_3} \quad (12)$$

The former corresponds to the method of moments and the resulting error is smaller than  $\pm 0.01$  for  $-1 < \kappa < 1/3$  ( $-2 < C_s < \infty$ ). The latter corresponds to the method of L-moments and the resulting error is smaller than  $\pm 0.008$  for  $-1 < \kappa < 1$  ( $-1/3 < \tau_3 < 1$ ).

The construction of linear probability plots is also easy if  $\kappa$  is fixed. It suffices to replace in the horizontal axis the Gumbel reduced variate  $z_H := -\ln(-\ln H)$  with the GEV reduced variate  $z_H := [(-\ln H)^{-\kappa} - 1] / \kappa$ . Such plots are portrayed in Figure 12 for the same distributions depicted in Figure 6 on Gumbel probability plots, but now for  $\kappa = 0.15$ . In addition to the empirical and EV2 distributions, upper and lower prediction limits of the former, computed by Monte Carlo simulation (e.g., Ripley, 1987, p. 176), have been plotted in this figure, which demonstrate the high uncertainty of estimates for large return periods.

## 8. Conclusions and discussion

The conclusions of this extensive analysis based on 169 rainfall series with lengths 100-154 years and a total number of 18 065 station-years from stations in Europe and USA may be summarized as follows.

1. Neither of the two-parameter special cases of the GEV distribution, i.e. the Gumbel and Fréchet distributions, is appropriate for modelling annual maximum rainfall series. On the contrary, the three-parameter EV2 distribution is a choice much closer to reality.
2. The shape parameter  $\kappa$  of the EV2 distribution is very hard to estimate on the basis of an individual series, even in series with length 100 years or more. This is because of the estimation bias and the large sampling variability of the estimators of  $\kappa$ , which was demonstrated here using simulation. For example, for sample size  $m = 30$  and  $\kappa = 0.15$  the method of moments estimates a  $\kappa$  almost zero and the method of L moments does not reject the false hypothesis of EV1 distribution at 75% of cases (see first part of the study). The analysis showed that even in the unified record with 18 065 values, the uncertainty in estimating  $\kappa$  is large as different estimation methods yield different estimates of  $\kappa$ . The

most important conclusion, however, is that the observed variability in the values of  $\kappa$  in the 169 series is almost entirely explained by statistical reasons as it is almost identical with the sampling variability. This allows the hypothesis that the shape parameter of the EV2 distribution is constant for all examined geographical zones, with value  $\kappa = 0.15$ .

3. The location parameter  $\psi$  of the EV2 distribution turned out to be fairly constant with a mean value  $\psi = 3.54$  (corresponding to  $\kappa = 0.15$ ) and coefficient of variation as low as 0.13. However, this small variation cannot be attributed to statistical reasons entirely as the sampling variation seems to be slightly lower than that observed in the 169 historical samples. This, however, is not a major problem as  $\psi$  can be estimated with relative accuracy on the basis of an individual series.
4. The scale parameter  $\lambda$  of the EV2 distribution varies with the station location and there is no need to seek a generalized law about it as it can be estimated with relative accuracy on the basis of an individual series.
5. The behaviour of the examined series over threshold turns out to be fully consistent with that of the annual maximum series, as the same parameter values of the EV2 distribution of the latter are equally good for the Pareto distribution of the former. Thus, the statistical analysis of either the annual maximum series or the series over threshold suffices to know the behaviour of both.
6. In engineering practice, the handling of the EV2 distribution can be as easy as that of the EV1 distribution if the shape parameter of the former is fixed to the value  $\kappa = 0.15$ . The parameter estimation is virtually the same (only some constants change) and very similar linear probability plots can be constructed (the Gumbel reduced variate  $z_H := -\ln(-\ln H)$  should be replaced with the GEV reduced variate  $z_H := [(-\ln H)^{-0.15} - 1] / 0.15$ , or in case of series over threshold with the Pareto reduced variate  $y_T := (T^{0.15} - 1) / 0.15$ . If the linearity of the plot is not necessary, a log-log plot of distribution quantile versus return period is a simpler choice.

In a recent study, Koutsoyiannis (1999) revisited Hershfield's (1961) data set (95 000 station-years from 2645 stations) and showed that this can be described by the EV2 distribution with  $\kappa = 0.13$ . The plot of Figure 13, indicates that the value  $\kappa = 0.15$  that is

proposed in the present study can be acceptable for that data set too. This enhances the trust that an EV2 distribution with  $\kappa = 0.15$  can be thought of as a generalized model appropriate for mid latitude areas of the north hemisphere. The present analyses do not confirm Hershfield's (1965) observation that arid areas tend to have higher relative extremes (ratios of maximum to mean or standard deviation) than areas with heavy rainfall, which as Koutsoyiannis (1999) showed, is equivalent to a negative correlation of  $\kappa$  with mean. Before a concrete conclusion on this issue can be drawn, long records from other geographical zones, especially tropical and south hemisphere ones, should be explored.

The results of this study also converge with other recent studies such as those by Chaouche (2001), Chaouche et al. (2002), Coles et al., (2003) and Sisson et al. (unpublished), which all verify the EV2/Pareto behaviour in the tail of the distribution of rainfall extremes and exclude the possibility of EV1/exponential behaviour. Particularly, Chaouche (2001) exploited a data base of 200 rainfall series of various time steps (month, day, hour, minute) from the five continents, each including more than 100 years of data. Using multifractal analyses he showed that (a) a Pareto type law describes the rainfall amounts for large return periods; (b) the exponent of this law is scale invariant over scales greater than an hour; and (c) this exponent is almost space invariant.

**Acknowledgements** The data from USA belong to the United States Historical Climatology Network (USHCN) and are available online from <http://lwf.ncdc.noaa.gov/oa/climate/research/ushcn/ushcn.html>. The data from the UK belong to the Land Surface Observation Data of the Met Office and were kindly provided through download from the web site <http://badc.nerc.ac.uk/> of the British Atmospheric Data Centre (BADC). The data from France were kindly provided by Philippe Bois (Laboratoire d'Etudes des Transferts en Hydrologie et Environnement, Ecole Nationale Supérieure d'Hydraulique et de Mécanique de Grenoble; LTHE-ENSHMG). The data from Italy were kindly provided by Alberto Montanari (University of Bologna). The record from Greece was originated from an earlier study (Koutsoyiannis and Baloutsos, 2000) and was updated with data values of the recent years kindly provided by Vasso Kotroni (National Observatory of Athens). Thanks are also due to Christian Onof (Imperial College) and Charles Obléd (LTHE-ENSHMG) for their help in seeking datasets from UK and France and for providing useful information and comments. With the editor's help, the paper was so fortunate as to bring two very encouraging, constructive and detailed reviews by Alberto Montanari and an anonymous reviewer, which improved the paper substantially.



## References

- Chaouche K. (2001) *Approche Multifractale de la Modelisation Stochastique en Hydrologie*, thèse, Ecole Nationale du Génie Rural, des Eaux et des Forêts, Centre de Paris (<http://www.engref.fr/thesechaouche.htm>).
- Chaouche, K., Hubert, P., Lang, G. (2002) Graphical characterisation of probability distribution tails, *Stochastic Environmental Research and Risk Assessment*, 16(5), 342-357.
- Chow V.T., Maidement D.R and Mays L.W.(1988), *Applied Hydrology*, McGraw-Hill, New York.
- Coles, S., Pericchi, L. R., and Sisson, S., (2003) A fully probabilistic approach to extreme rainfall modeling, *Journal of Hydrology*, 273(1-4), 35-50.
- Hershfield, D. M. (1961) Estimating the probable maximum precipitation, *Proc. ASCE, J. Hydraul. Div.*, 87(HY5), 99-106.
- Hershfield, D. M. (1965) Method for estimating probable maximum precipitation, *J. American Waterworks Association*, 57, 965-972.
- Hosking, J. R. M. (1990) L-moments: Analysis and estimation of distributions using linear combinations of order statistics, *J. R. Stat. Soc., Ser. B*, 52, 105-124.
- Jenkinson, A. F. (1955) The frequency distribution of the annual maximum (or minimum) value of meteorological elements, *Q. J. Royal Meteorol. Soc.*, 81, 158-171.
- Jenkinson, A. F. (1969) Estimation of maximum floods, *World Meteorological Organization, Technical Note No 98*, ch. 5, 183-257.
- Koutsoyiannis, D. (1999) A probabilistic view of Hershfield's method for estimating probable maximum precipitation, *Water Resources Research*, 35(4), 1313-1322.
- Koutsoyiannis, D., and Baloutsos, G. (2000) Analysis of a long record of annual maximum rainfall in Athens, Greece, and design rainfall inferences, *Natural Hazards*, 22(1), 31-51.
- National Research Council (1994) *Estimating Bounds on Extreme Precipitation Events*, National Academy Press, Washington.
- Ripley, B. D. (1987) *Stochastic Simulation*, Wiley, New York.
- Sisson, S. A., Pericchi, L. R., and Coles, S. (unpublished) A case for a reassessment of the risks of extreme hydrological hazards in the Caribbean ([www.maths.unsw.edu.au/~scott/papers/paper\\_caribbean\\_abs.html](http://www.maths.unsw.edu.au/~scott/papers/paper_caribbean_abs.html))
- Turcotte, D. L. (1994) Fractal theory and the estimation of extreme floods, *J. Res. Natl. Inst. Stand. Technol.*, 99(4), 377-389.

**Table 1** General characteristics of raingauges of the different geographical zones.

		Geographical zone						Total
		1	2	3	4	5	6	
Number of stations		104	19	15	3	24	4	169
Record length	min	100	100	100	100	100	128	100
	max	130	131	122	103	130	154	154
Number of station-years		10942	2012	1610	304	2624	573	18065
Elevation (m)	min	3	3	11	376		6	3
	max	1867	917	2078	1870		107	2078

**Table 2** General characteristics of the top ten, in terms of record length, raingauges.

Name	Zone/Country /State	Latitude (°N)	Longitude (°)	Elevation (m)	Record length	Start year	End year	Years with missing values
Florence	6/Italy	43.80	11.20	40	154	1822*	1979	1874-77
Genoa	6/Italy	44.40	8.90	21	148	1833	1980	
Athens	6/Greece	37.97	23.78	107	143	1860	2002	
Charleston City	2/USA/SC	32.79	-79.94	3	131	1871	2001	
Oxford	5/UK	51.72	-1.29		130	1853	1993	1930, 1933, 1961-69
Cheyenne	1/USA/WY	41.16	-104.82	1867	130	1871	2001	1877
Marseille	6/France	43.45	5.20	6	128	1864	1991	
Armagh	5/UK	54.35	-6.65		128	1866	1993	
Savannah	2/USA/GA	32.14	-81.20	14	128	1871	2001	1969-71
Albany	1/USA/NY	42.76	-73.80	84	128	1874	2001	

\* Record starts in 1813 but values prior to 1822 are incorrect.

**Table 3** Averages and ranges of statistical characteristics of annual maximum daily rainfall series for the different geographical zones.

		Geographical zone						Total
		1	2	3	4	5	6	
Sample mean, $\mu$ (mm)	min	34.2	65.3	19.1	31.8	31.3	48.5	19.1
	mean	65.7	91.0	36.5	39.4	36.1	68.9	61.4
	max	90.1	109.0	75.3	48.7	46.4	110.9	110.9
Sample maximum, $x_{\max}$ (mm)	min	88.4	146.8	40.1	84.3	54.1	140.0	40.1
	mean	175.8	265.7	83.9	125.2	89.7	225.4	165.8
	max	429.5	490.0	157.0	201.2	130.3	389.2	490.0
Coefficient of variation, $C_v$	min	0.26	0.32	0.31	0.35	0.26	0.35	0.26
	mean	0.38	0.42	0.36	0.41	0.34	0.42	0.38
	max	0.68	0.57	0.47	0.47	0.45	0.48	0.68
Coefficient of skewness, $C_s$	min	0.58	0.89	0.83	1.08	0.55	1.65	0.55
	mean	1.69	1.81	1.19	1.93	1.70	1.92	1.67
	max	4.94	3.89	1.69	3.32	3.22	2.03	4.94
L-coefficient of variation, $\tau_2$	min	0.14	0.18	0.16	0.19	0.14	0.18	0.14
	mean	0.19	0.21	0.19	0.21	0.17	0.22	0.19
	max	0.26	0.25	0.25	0.22	0.22	0.24	0.26
L-coefficient of skewness, $\tau_3$	min	0.12	0.16	0.14	0.16	0.15	0.22	0.12
	mean	0.24	0.26	0.21	0.23	0.24	0.26	0.24
	max	0.43	0.38	0.26	0.29	0.35	0.28	0.43

**Table 4** Averages over all raingauges and dispersion characteristics of the parameters of the GEV distribution as estimated by three different methods from the annual maximum daily rainfall series.

Parameter		Estimation method		
		Max likelihood	Moments	L-Moments
$\kappa$	Mean	0.103	0.052	0.103
	Standard deviation	0.080	0.079	0.085
	Min	-0.061	-0.121	-0.080
	Max	0.303	0.238	0.373
	Percent positive	91%	74%	92%
$\lambda$	Mean	15.39	16.64	15.52
	Standard deviation	5.63	6.31	5.81
	Min	4.95	5.16	4.86
	Max	31.08	34.89	32.13
$\psi$	Mean	3.36	3.14	3.34
	Standard deviation	0.42	0.44	0.43
	Min	2.54	2.07	2.42
	Max	4.48	4.44	4.47

**Table 5** Parameters of the EV2 distribution as estimated by four different methods from the unified record of all 169 annual maximum rescaled daily rainfall series (18 065 station-years).

Parameter	Estimation method			
	Max likelihood	Moments	L-moments	Weighted least squares
$\kappa$	0.093	0.126	0.104	0.148
$\lambda$	0.258	0.248	0.255	0.236
$\psi$	3.24	3.36	3.28	3.54

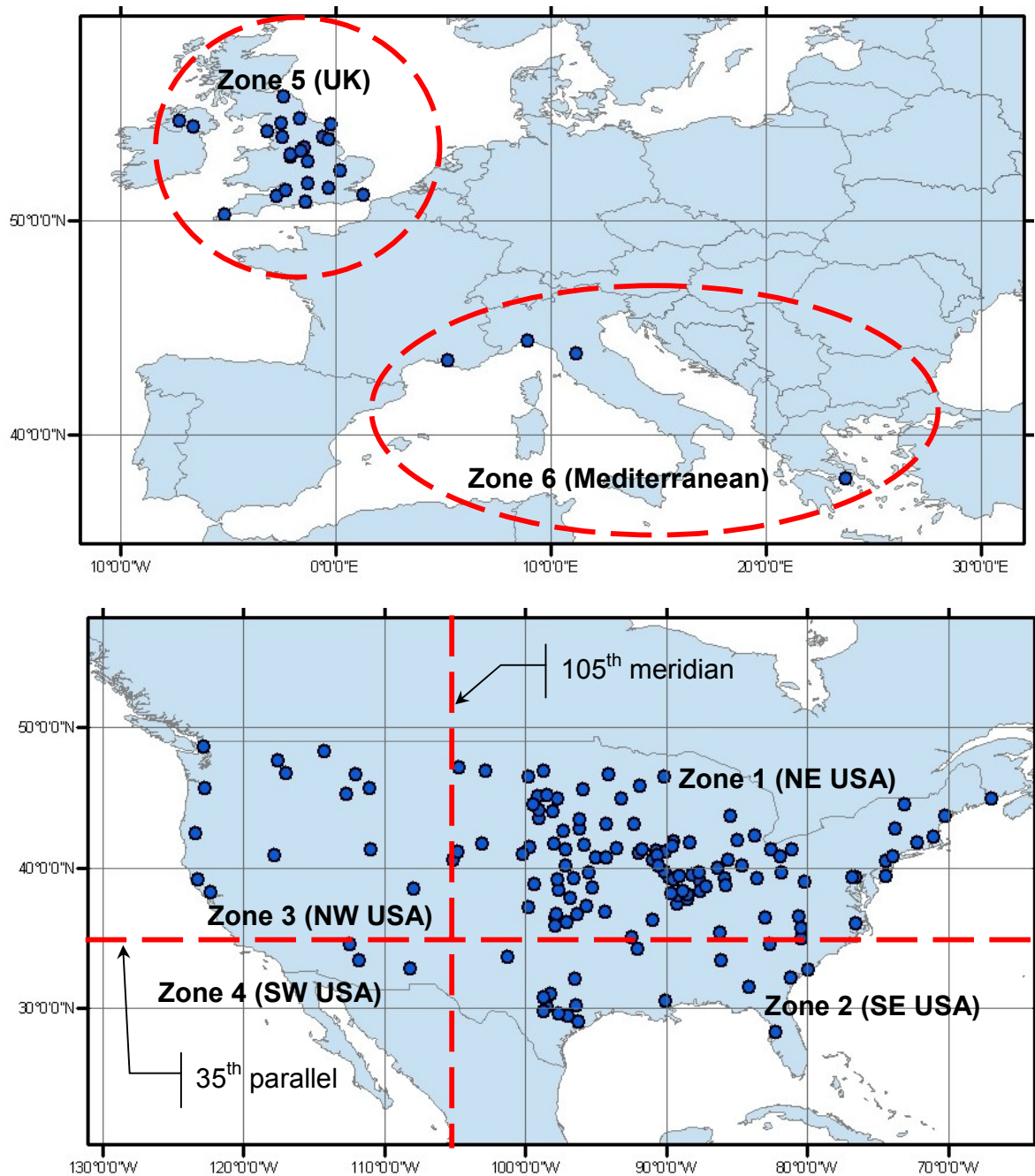


**Figure 1** Geographical locations of rain gauges.

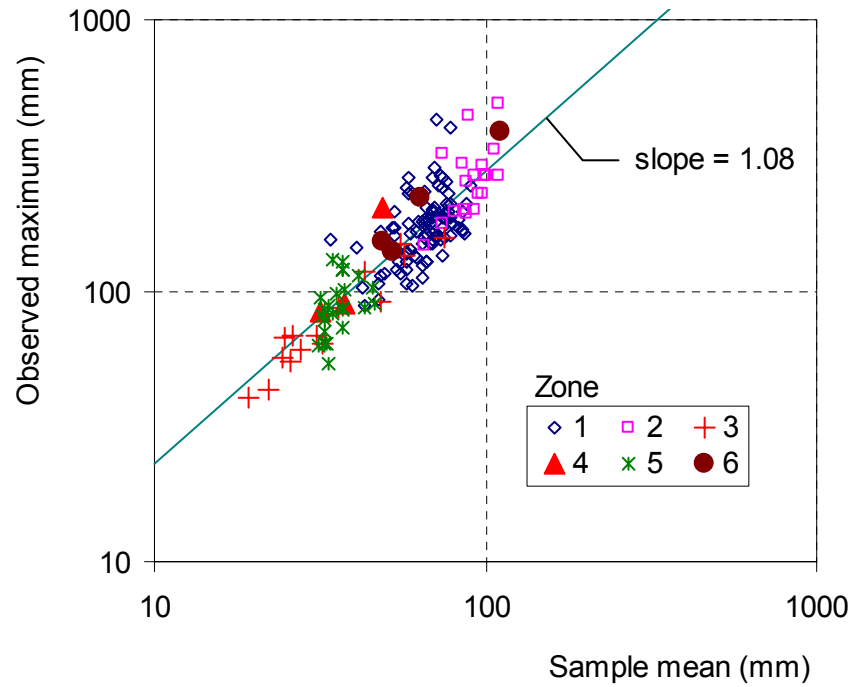


**Figure 2** Plot of the sample mean and maximum, over the observation period, of each annual maximum daily rainfall series for the six different geographical zones.

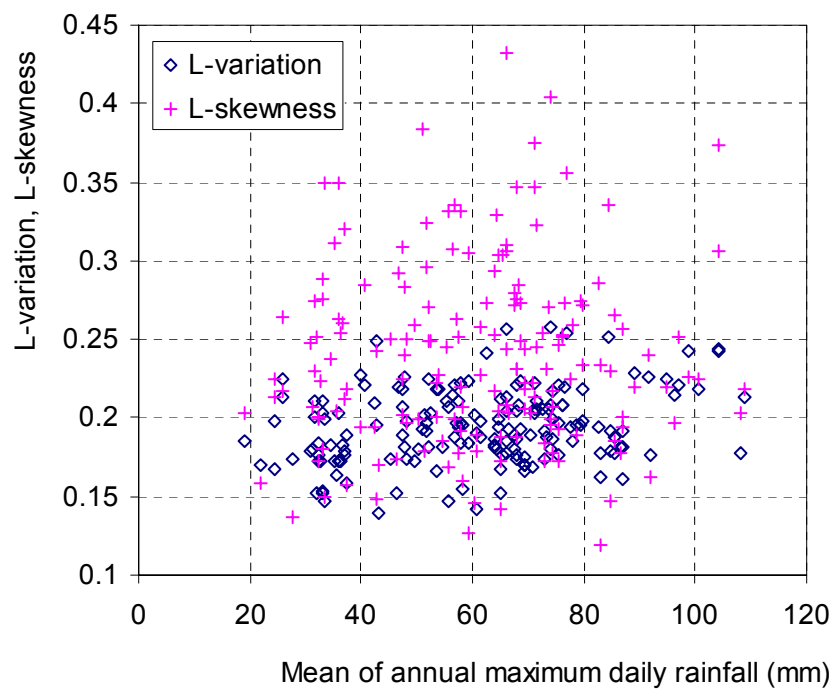


**Figure 3** Plot of the L-variation and L-skewness coefficients vs. the mean of the annual maximum daily rainfall series.

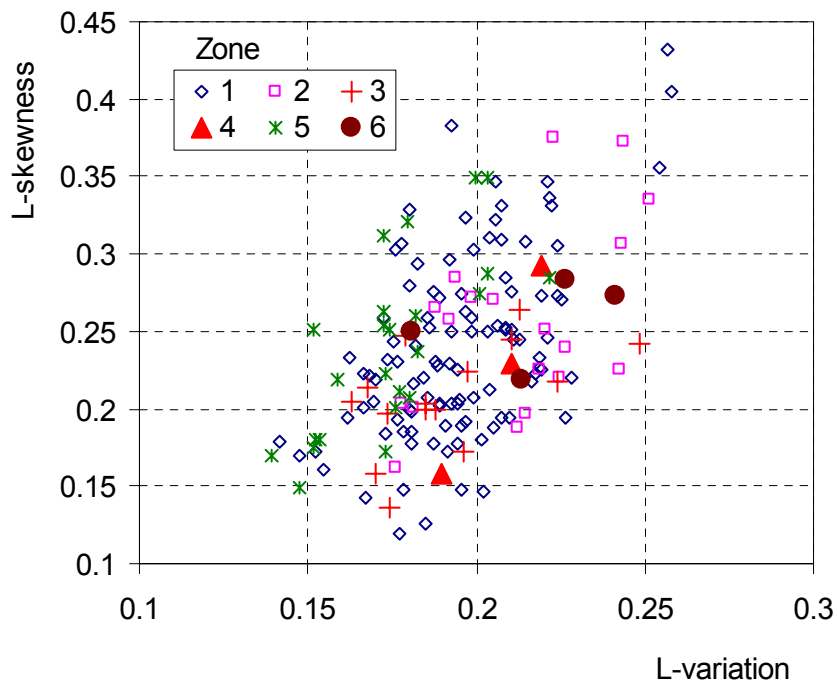


**Figure 4** Plot of L-skewness vs. L-variation coefficient for the annual maximum daily rainfall series for the six different geographical zones.

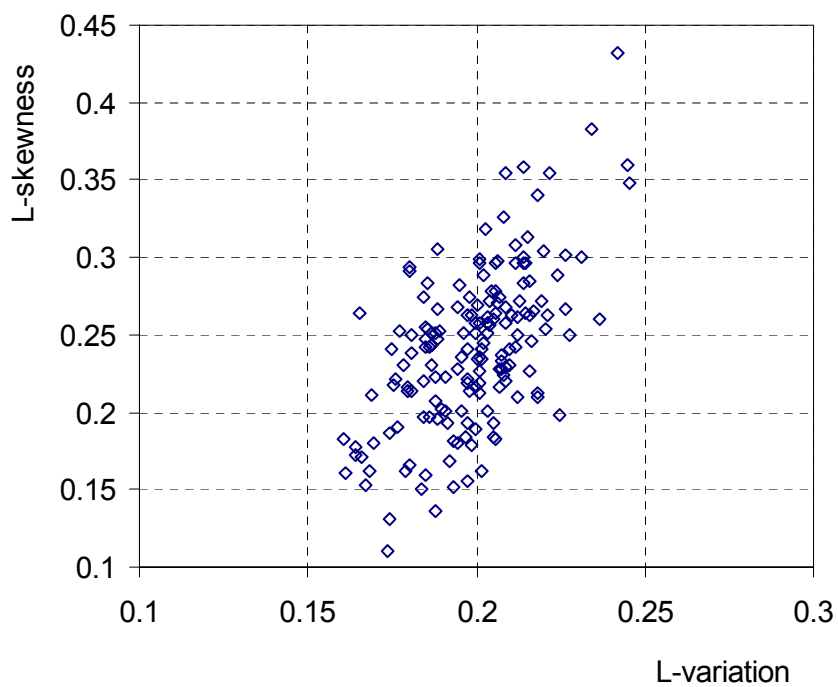


**Figure 5** Plot of L-skewness vs. L-variation coefficient for 169 synthetic samples with lengths and means equal to those of the historical records, generated from the EV2 distribution with shape parameter  $\kappa = 0.103$  and location parameter  $\psi = 3.34$ .

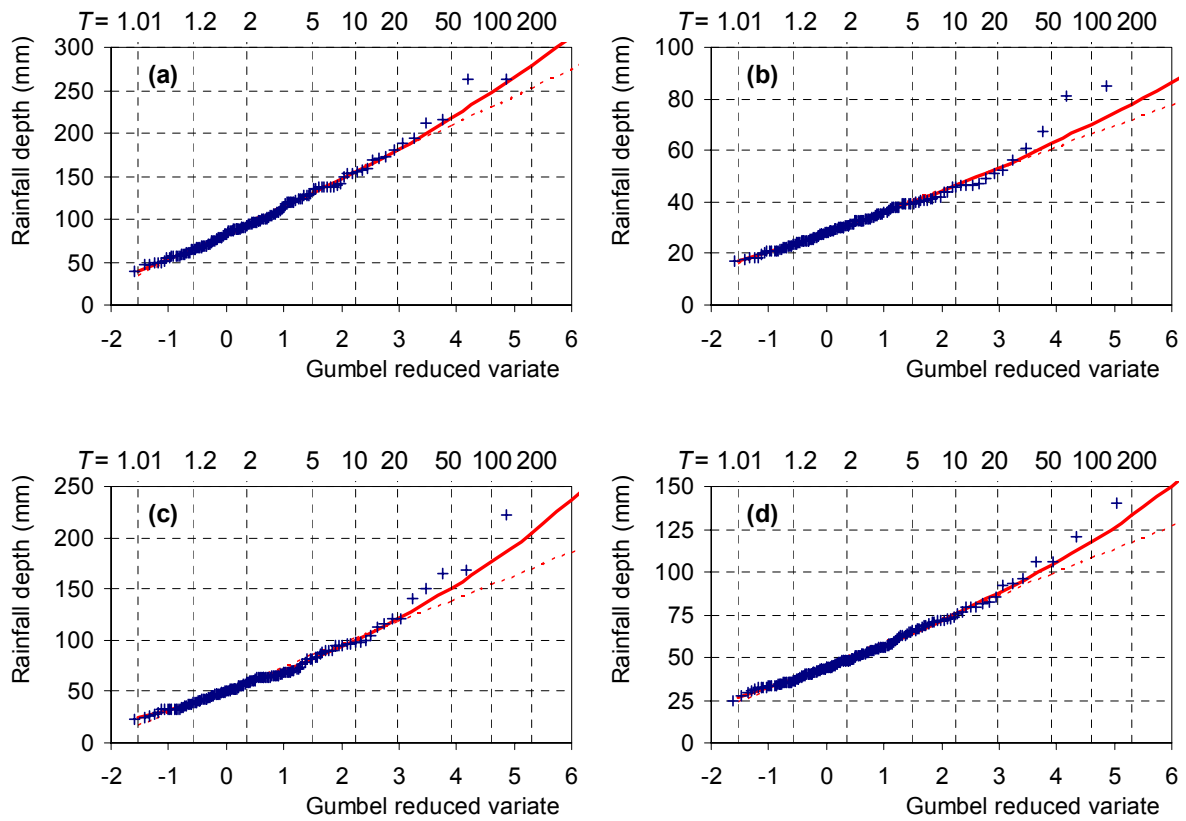


**Figure 6** EV2 (continuous lines) and EV1 (dotted lines) distributions fitted by the method of L-moments and comparison with the empirical distribution (crosses) for the annual maximum daily rainfall series of (a) Charleston City, USA/SC; (b) Oxford, UK (c) Marseille, France; and (d) Florence, Ximeniano Observatory, Italy (Gumbel probability plots).



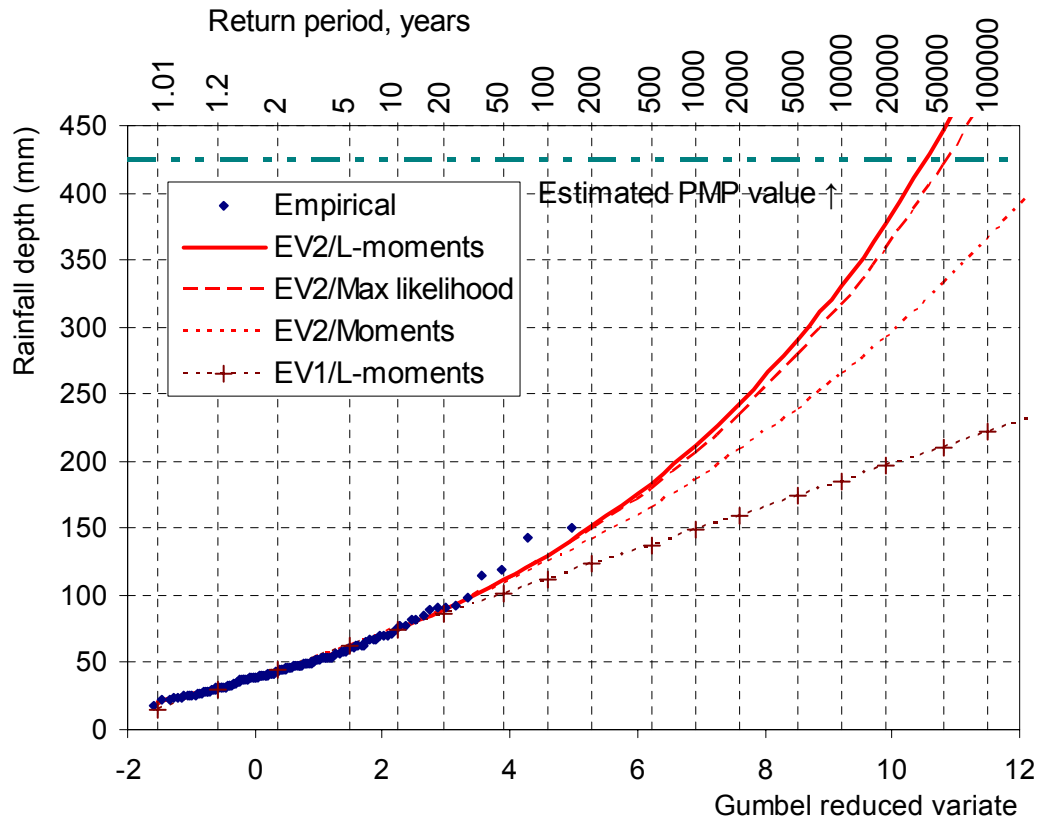


**Figure 7** EV2 and EV1 distributions fitted by several methods and comparison with the empirical distribution for the annual maximum daily rainfall series of Athens, National Observatory, Greece (Gumbel probability plot). The PMP value (424.1 mm) was estimated by Koutsoyiannis and Baloutsos (2000).

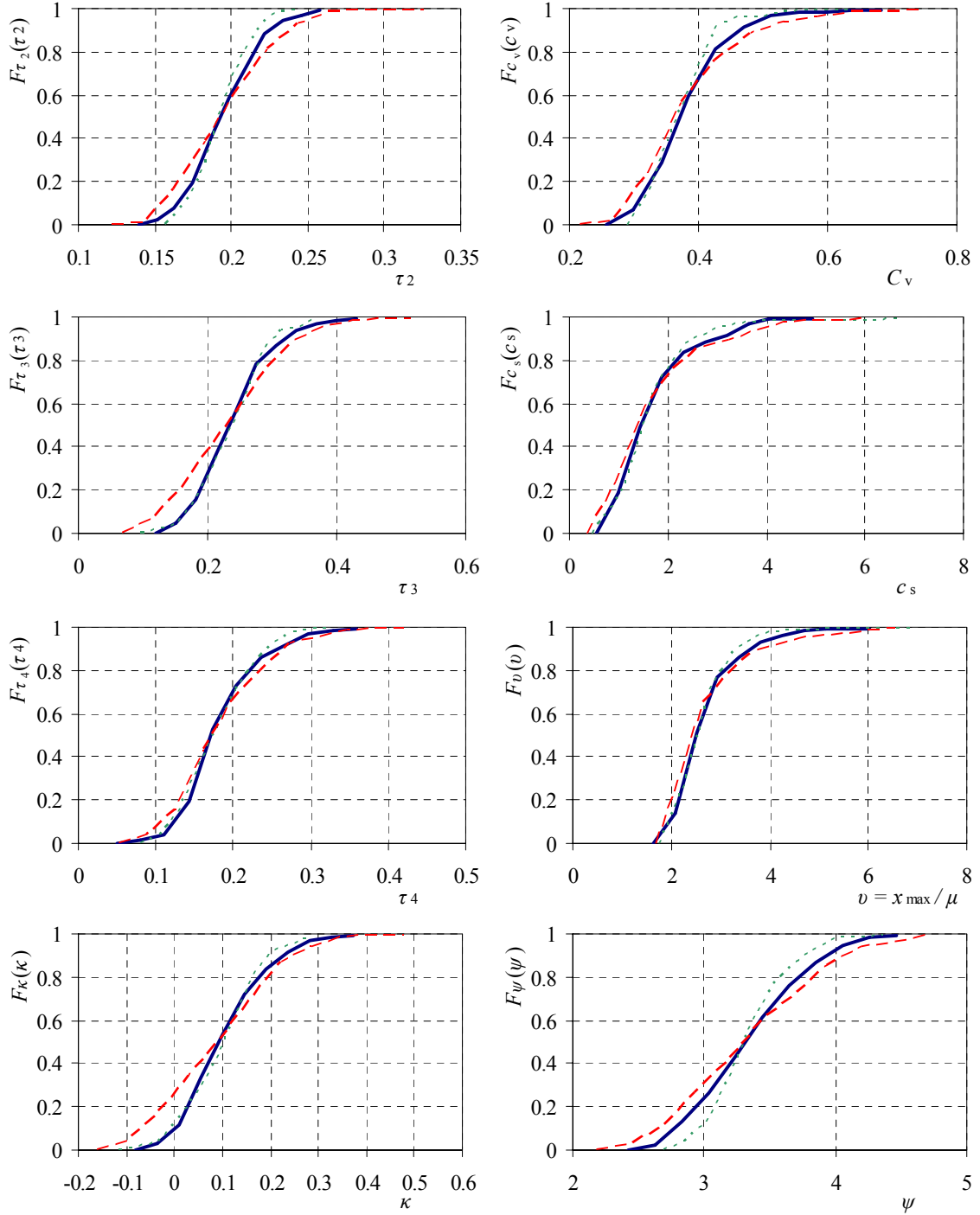


**Figure 8** Empirical distribution functions of several dimensionless sample statistics (coefficients of variation  $\tau_2$  and  $C_v$ , skewness  $\tau_3$  and  $C_s$ , and kurtosis  $\tau_4$ ; ratio of maximum value  $x_{\max}$  to mean value  $\mu$ ; and L-moments estimates of parameters  $\kappa$  and  $\psi$  of the GEV distribution), as computed from either: the 169 historical annual maximum daily rainfall series (thick continuous lines); 169 synthetic samples with lengths and means equal to those of historical series generated from the GEV distribution with constant shape parameter  $\kappa = 0.103$  and location parameter  $\psi = 3.34$  (dotted lines); and 169 synthetic samples with lengths and means equal to those of historical series generated from the GEV distribution with shape parameter  $\kappa$  and location parameter  $\psi$  varying following uniform distributions (dashed lines).

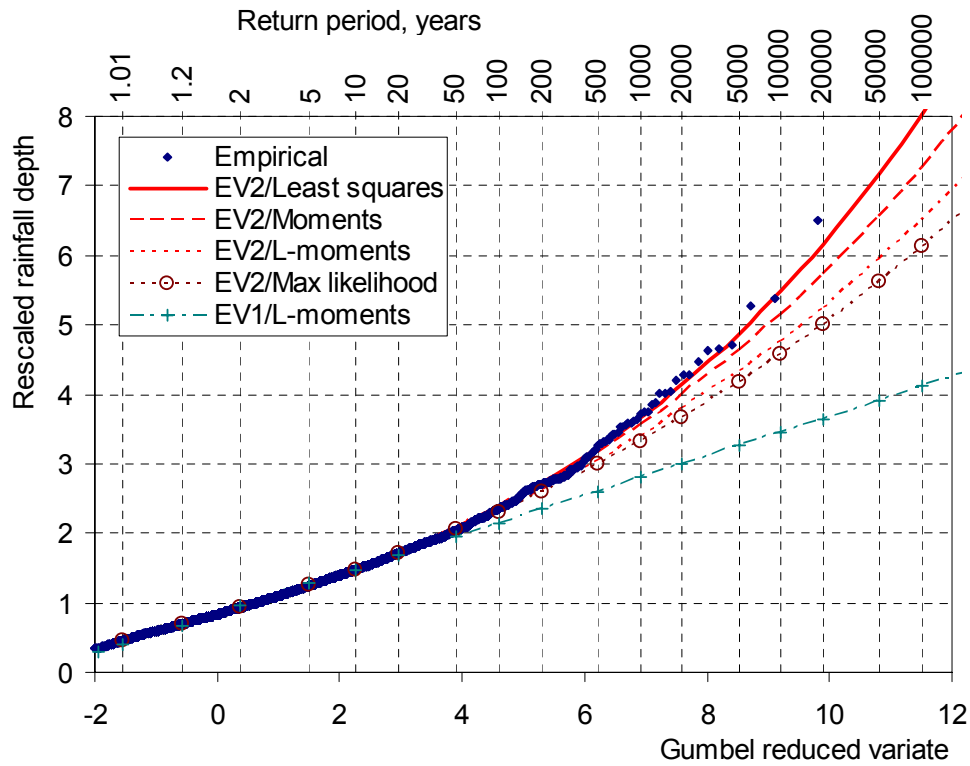


**Figure 9** EV2 and EV1 distributions fitted by several methods and comparison with the empirical distribution for the unified record of all 169 annual maximum rescaled daily rainfall series (18 065 station-years).

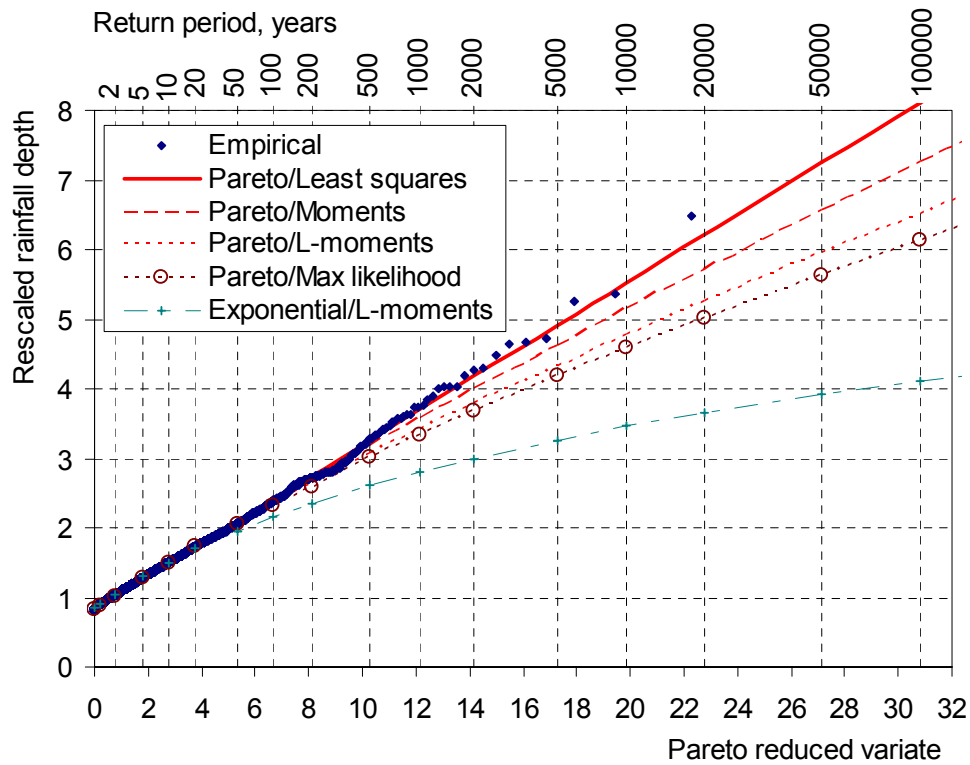


**Figure 10** Empirical distribution of the union of the 168 series of rescaled rainfall depths over threshold (17922 station-years) in comparison with the Pareto distribution with parameters estimated from the unified series of annual maxima, shown in Table 5 (Pareto probability plot with  $\kappa = 0.15$ ).

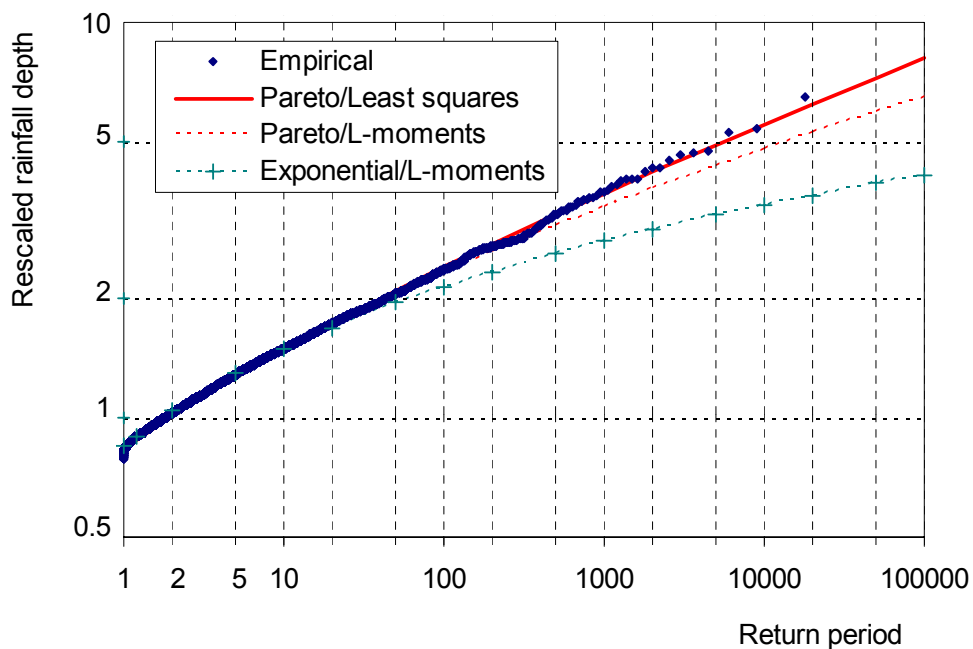


**Figure 11** Empirical and Pareto distributions of the union of the 168 series of values over threshold (17922 station-years) as in Figure 10 but in a double logarithmic plot of rescaled rainfall depths vs. return period.

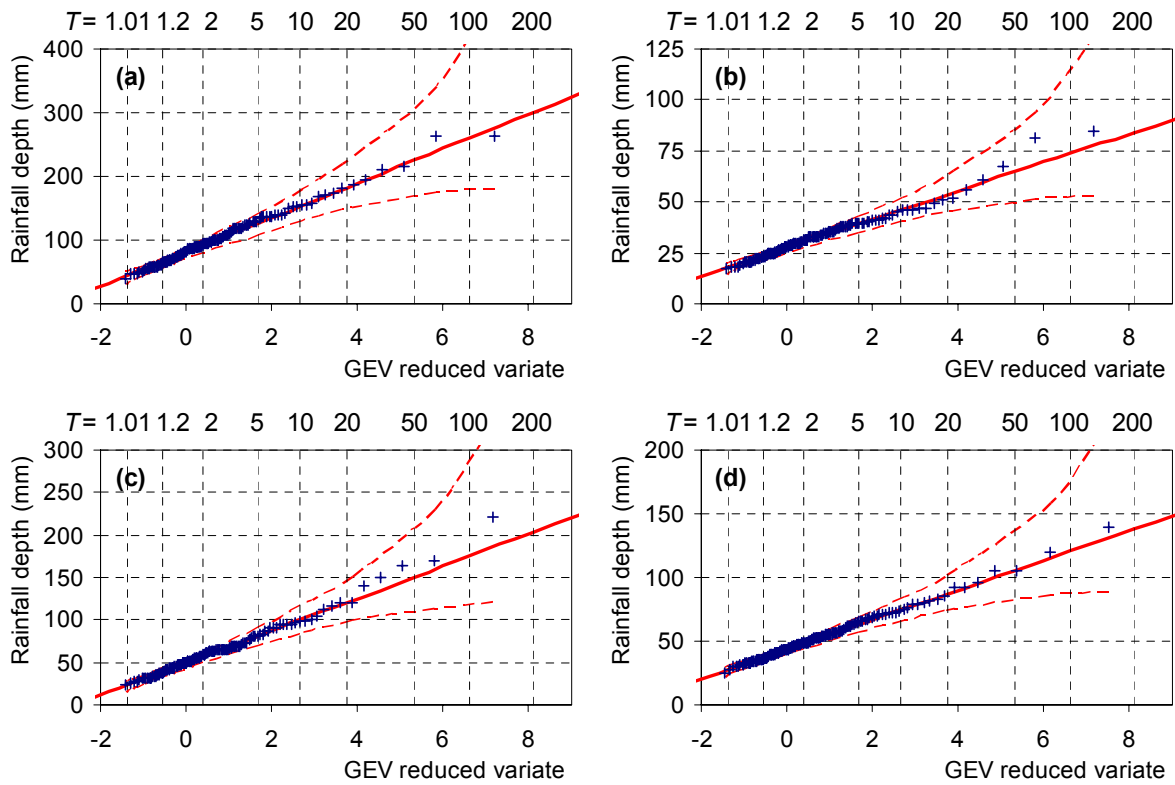


**Figure 12** Empirical distributions (crosses), EV2 distributions (continuous lines), and 95% Monte Carlo prediction limits for the empirical distribution (dashed lines) of the annual maximum daily rainfall series of (a) Charleston City, USA/SC; (b) Oxford, UK (c) Marseille, France; and (d) Florence, Italy, as in Figure 6 but in GEV plot with  $\kappa = 0.15$ . The EV2 distribution was fitted by the method of L-moments assuming fixed  $\kappa = 0.15$ .

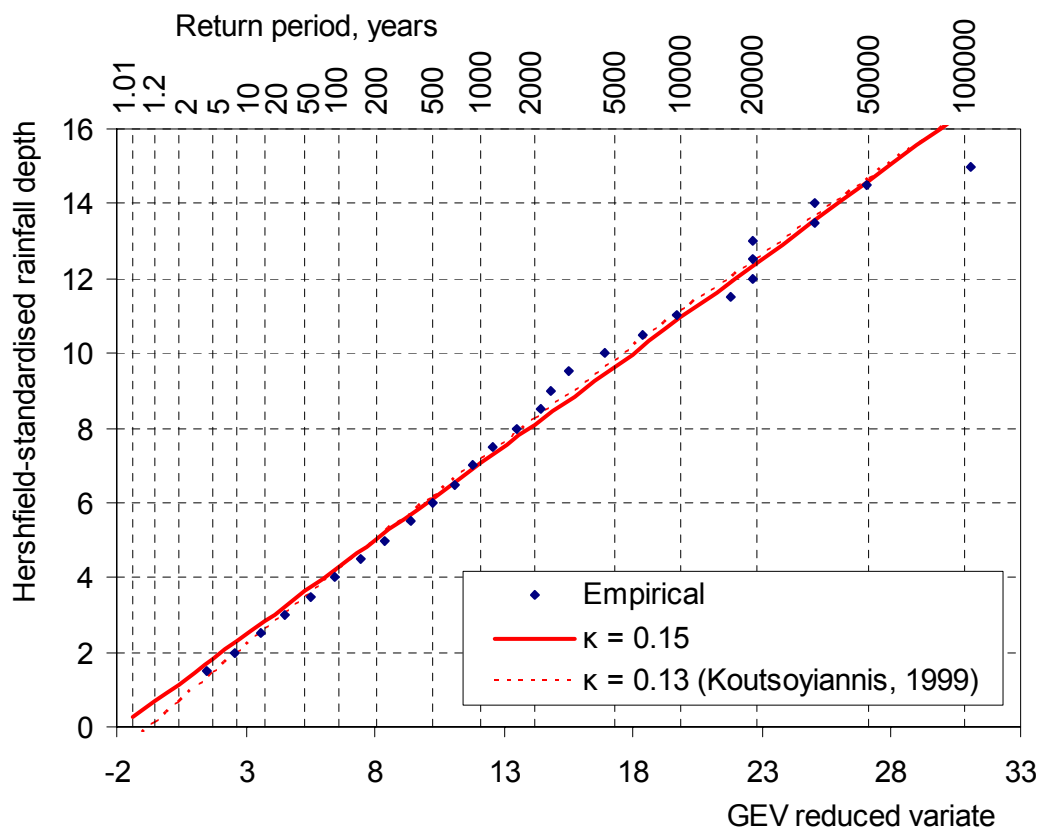


**Figure 13** Empirical distribution of standardized rainfall depth  $k$  for Hershfield's (1961) data set (95 000 station-years from 2645 stations), as determined by Koutsoyiannis (1999), and fitted EV2 distributions with  $\kappa = 0.13$  (Koutsoyiannis, 1999) and  $\kappa = 0.15$  (present study) (GEV probability plots with  $\kappa = 0.15$ ).